P 1853

Laboratory of Nuclear Problems,
Joint Institute for Nuclear Research, Dubna

Report no. P 1853

# An increase of the internal beam current of the JINR synchro-cyclotron by additional electrostatic focusing

V.I. Danilov, I.B. Enchevich, B.N. Marchenko
E.A. Polferov, A.N. Safonov, A.V. Shestov

Translated at CERN by J. Rice and N. Mouravieff

DUBNA 1964

# AN INCREASE OF THE INTERNAL BEAM CURRENT OF THE JINR SYNCHRO-CYCLOTRON BY ADDITIONAL ELECTROSTATIC FOCUSING

V.I. Danilov, I.B. Enchevich, B.N. Marchenko,
E.A. Polferov, A.N. Safonov, A.V. Shestov

Limitation of the current of ions being accelerated in the synchro-cyclotron under optimum ion capture conditions in acceleration and in the absence of phase losses in the acceleration process is mainly dependent on the defocusing action of the space charge of the ion bunch in the 25 - 30 cm diameter region surrounding the ion source. The presence of a large space charge is explained by the fact that at a comparatively low accelerating voltage ($U_{acc} \leq 20$ kV) and in the absence of a slit system, the beam radius is extended in very short steps of approximately 1 mm [1], the radius of the first revolution not exceeding 3 mm, which makes it impossible to use closed-type ion sources.

In the central region the forces of Coulomb ion scattering in the beam prove to be considerably greater than the focusing forces, which are due to the decrease of the magnetic field along the radius. As a result, the vertical stability of the beam is disturbed and considerable particle losses arise, until the beam reaches the region where the defocusing forces of the space charge, which decrease as a result of the particle losses and the increase in volume occupied by the beam, become less than the magnetic focusing forces which grow with the radius.

In order to cut down particle losses and thereby to increase the beam current, it is necessary to increase near the centre of the accelerator the forces which focus the beam in the vertical direction. To increase the magnetic focusing forces, it is necessary to ensure a further decrease of the magnetic field along the radius, since the magnetic focusing forces are proportional to n, where

$$n = -\frac{r}{B} \times \frac{dB}{dr}$$

is the non-uniformity factor of the magnetic field. Data are available concerning the increase in the beam current of the 184-inch synchro-cyclotron at Berkeley by further decreasing the magnetic field[2]. However, with the large aperture of the JINR synchro-cyclotron chamber, namely 60 cm, the increase of n for small radii up to r = 10 ÷ 15 cm is made difficult by the actual design of the ion source. Installing on the cover plates of the chamber iron shims of dimensions $\Delta h$ = 2.5 cm, $\Delta r$ = 3.7 cm and $r_{cp}$ = 17.4 cm did not lead to an increase of current, as a noticeable increase of n begins with radii bigger than r = 11 ÷ 12 cm. Besides that a change of n leads to a change in the initial phase conditions, since the frequency range of the accelerating voltage, at which particles are captured for acceleration, depends on the decrease of the magnetic field[1]. Thus, when the vertical focusing near the centre is increased by greatly reducing the magnetic field, it is necessary to find again the optimum capture conditions and in accordance with them to correct the frequency programme of the synchro-cyclotron.

Vertical beam focusing at small radii can also be increased by creating around the ion source an electrostatic field with its vertical intensity components directed towards the median plane. Thus, for example, focusing action in the vertical direction can be caused by an electrostatic field, which is formed by the negative voltage put into the dee for improving the operation of the r.f. generator. Keller, Fidecaro and Barbier have given approximate calculations of the focusing action of a negative voltage on the dee in the CERN synchro-cyclotron[3]. In these calculations the influence of the ion-source column on the field distribution is not taken into account, since in the CERN synchro-cyclotron the source only works during ion capture. In this case the focusing action is maximum at the centre of the accelerator and decreases towards zero when r = 12 ÷ 13 cm.

However, the dependence of the focusing action of the negative voltage supplied to the dee on the radius in the JINR synchro-cyclotron is of a slightly different nature, since the distribution of the electric field of the dee in the central region is strongly influenced by the plasma

column of the ion source, which exists during the entire acceleration period[4]. As a result of this, the focusing action of the shift does not reach maximum in the centre of the machine, but falls to zero at the plasma limit of the arc discharge. The effect of the negative voltage applied to the dee on the intensity of the proton beam in the JINR synchro-cyclotron is shown in Fig. 1.

In the JINR synchro-cyclotron the absence of a counter-dee frame creates favourable possibilities for the formation of an additional electrostatic field, focusing the beam in the vertical direction.

To create an additional electrostatic field with a vertical intensity component in the central region two semi-circular electrodes were used, placed against the dee symmetrically in relation to the median plane. When supplying them with negative voltage, an electrostatic field is formed in the space between the dee and the electrodes around the ion source column. This field has a focusing action, analogous to the action of the negative voltage on the dee. The shape of the additional electrostatic field was studied by simulating in an electrolytic bath the central part of the accelerating chamber with the dee, the ion source and the focusing electrodes[4]. For this purpose it was assumed that the plasma column of the ion source is under the earth potential.

Figure 2 shows the distribution of the potential in the median plane of the synchro-cyclotron near the centre; 1.7 kV negative voltage is supplied to the dee and 12.5 kV to the electrodes. To find the vertical components of the additional electrostatic field, measurements of the dependence of the potential on z were carried out in an electrolytic bath, with a co-ordinate grid for several values of the orbit radius r and the azimuth $\Phi$, reckoned from the perpendicular running from the centre towards the dee[4]. The vertical forces were calculated with the formula:

$$F_z(r,\Phi) = - e \frac{du(z,r,\Phi)}{dz} ,$$

where $u(z,r,\Phi)$ = the dependence of the potential on the distance to the median plane for the values r and $\Phi$, given by the co-ordinate grid. Figure 3 shows graphs of the additional focusing forces acting on the protons at a distance of 4.5 cm from the median plane when 12.5 kV negative voltage is supplied to the electrodes. For that purpose the electrodes are situated at a distance of 15 cm from the centre of the accelerator. Peaks on the curves in the region of the azimuth $\Phi = 70 - 80^{\circ}$ and $\Phi = 280 - 290^{\circ}$ for the radii of the orbits, beginning with r = 10 cm, are explained by the effect of the dee on the shape of the electrostatic field, since in the region of these azimuths the orbits cut the edge of the dee. The dip of the focusing force around the azimuth $\Phi = 180^{\circ}$ for r = 14 cm is due to the orbits entering the defocusing region of the additional electrostatic field.

The vertical forces of the additional electrostatic field, averaged at the azimuth and depending on the orbit radius, are shown in Fig. 4. It should be noted that the effect of the first harmonic of the focusing forces, as is shown by the estimates made, may be disregarded. For comparison, a graph is also drawn in Fig. 4 of the magnetic focusing forces, acting on protons at the same distance from the median plane.

Additional focusing forces, exceeding magnetic forces in small radii, reduce the divergence of the beam in the vertical direction under the action of the Coulomb scattering forces. As a result there is an increase in the number of particles reaching the radii, where the sum of the additional electrostatic forces and the magnetic focusing forces exceeds the Coulomb scattering forces. At radii greater than 15 cm the additional electrostatic field has a defocusing effect on the beam, as can be seen in Fig. 4. However, at these radii the magnetic focusing forces are considerably greater than the electrostatic, and the vertical stability of the beam is not affected.

The layout of the focusing electrodes in the acceleration chamber is shown in Fig. 5, and a photograph of it is given in Fig. 6. The electrodes are placed against the dee. They are firmly fastened with the aid of

steatite insulators to plates which are connected to carriages. The carriages can be moved perpendicularly to the edges of the dee along guides attached to the cover plates of the chamber. The plates, the carriages and the guides are made of aluminium alloy (duraluminium). The distance between the electrodes can be altered by means of the screws fixing the carriages to the plates. The movable parts of the screen can be moved in a vertical direction and serve to shape the focusing electrostatic field in the space between the dee and the focusing electrodes. Figure 5 gives the characteristic direction of two lines of force - one from the dee to the electrodes, the other from the screen to the electrodes - when negative voltage is supplied to the electrodes. Condensors with a total capacity of 0.01 microfarad at $U_{operating}$ = 27 kV earth the electrodes at r.f. voltage. The construction of the fastening of the condensors between the plates and the electrodes allows them to be quickly replaced in the event of their failure, which is essential from the point of view of minimum radiation of the operating staff. The voltage is fed to the focusing electrodes by means of two feeders with quartz-tube insulation placed inside the chamber. The top and bottom electrodes have separate lead-ins to the vacuum chamber through steatite insulators.

Experimental relationships, obtained from examination of the focusing device, confirm the existence of the limiting action of the space charge on the internal beam current in the synchro-cyclotron.

Figure 7 shows the dependence of the proton beam intensity at the final radius on the focusing voltage $U_f$ at various flow rates of hydrogen fed to the ion source at zero arc voltage. In the JINR synchro-cyclotron a cold cathode ion source is used. When a small quantity of gas is supplied, the majority of the ions that have been formed are captured for acceleration. Since the value of the space charge is not high and its scattering effect is small, the relative increase of the beam current as a result of the action of the focusing field of the electrodes is small. A sharp decrease in the beam intensity for the case of a gas flow rate of 3 $cm^3$/min with an increase of $U_f$ is explained by the fact that the ion source stops working at zero arc voltage. With the increase in the quantity of hydrogen fed to the ion

source there is an increase in the total number of ions and, consequently, the number of protons captured for acceleration, and in the charge density of the beam. The additional beam current is increased when a negative voltage is supplied to the electrodes since the increased beam density leads to an increase in the defocusing action of the space charge. At the same time a higher voltage on the focusing electrodes is required in this case to compensate for the defocusing forces. This process is continued until, owing to the increased density of the gas in the central region of the accelerator, losses caused by scattering on the gas result in a reduction of the beam current. The maximum current increase, owing to focusing at various gas flow rates, is shown in percentages on the curves of Fig. 7.

Figure 8 gives similar dependences, where the arc voltage of the ion source is chosen as an additional parameter. The dependence of the intensity on the arc voltage is fairly weak.

The dependence of the beam intensity at the final radius on the focusing voltage $U_f$ for various values of the accelerating voltage supplied to the dee is shown in Fig. 9. It can be seen that when the amplitude of the accelerating voltage is small, the focusing action of the booster electrodes is small, since in this case too, because of the small number of protons captured for acceleration, the charge density in the beam is small, and in practice it does not lead to beam losses due to Coulomb scattering forces. With the increase in the accelerating voltage the charge density in the beam rises and current losses owing to Coulomb scattering can be offset by electrostatic focusing. The relative intensity increase through the action of electrostatic focusing is indicated on the appropriate curves. With the rise in the accelerating voltage the relative intensity increase becomes greater, and the maximum shifts towards large values of the focusing voltage.

Figure 10 gives the dependence of the beam current on the focusing voltage $U_f$ fed to the electrodes at various values of the negative voltage $U_d$ on the dee. It can be seen that with the rise of $U_d$ the optimum shifts slightly towards the higher values of $U_f$. The relative rise in intensity is greater at lower values of $U_d$. At zero focusing voltage electrostatic focusing is only created by negative voltage on the dee.

As a consequence of the alteration in the direction of the vertical electrostatic forces, by supplying reversed polarity (+) voltage to the electrodes, the beam current is lowered. Figure 11 shows the dependence of the proton current at a radius of 60 cm on the value and sign of the voltage fed to the focusing electrodes. It should be noted that with positive polarity an accelerator operation stability can be attained in the reduced intensity operating conditions required for some experiments. Before this method was used, reduced intensity was obtained through decreasing the accelerating voltage and gas flow rate, and any considerable decrease (more than 100 times) in beam current was limited by the unstable operation of the ion source.

Figure 12 shows the dependence of the proton beam intensity on the focusing voltage for several distances between the edge of the dee and the focusing electrodes. The rise in beam current with the increase of the gap between the dee and the electrodes is connected with the extension of the focusing region (see Fig. 5). The voltage growth, at which the beam current is maximum, is also regular - the value of the vertical component of the electrostatic field density required for focusing must remain constant. When the gap is increased, this is obtained by increasing the voltage. The presence of the optimum focusing effect due to the voltage value $U_f$ is connected with the effect on the charged particle beam of the horizontal component of the electrostatic field, which causes orbit drift. This leads to losses at the beginning of the acceleration of the particles making larger radial phase oscillations. It is known that the frequencies at which these particles can be captured are near the upper limit of the capture frequency range[1]. Measurement of the capture time in relation to $U_f$, produced by means of gradually cutting off the frequency programme on the higher frequency side, effectively shows that with an increase in $U_f$ the upper limit of the capture frequency range is moved towards the lower frequencies (see Fig. 13). The lower limit also moves slightly towards the lower frequencies, since particles, which before were lost because the energy was received too quickly (i.e. the phase velocity was too high), acquire smaller phase velocity as a result of drift and precession, and do not escape from the acceleration process. The reduction of capture

time which is observed when $U_f$ increases (see Fig. 14) is mainly due to losses of particles which produce larger radial phase oscillations. The current rise because of the increase in vertical focusing when $U_f$ increases, prevails at the beginning over the losses of particles which are captured near the upper limit of the stability region, and the beam intensity grows. With further increase of $U_f$, increasing losses of particles with large radial phase oscillation amplitude cause reduced beam current.

The influence of the focusing voltage on the time structure of the particle beam is shown in Fig. 15. From this figure it can be seen that the pulse duration of the beam at the final radius increases by approximately 20%.

The change in the curvature of the lines of force, ending on the screens, explains the dependence of the focusing action of the device on the gap between the electrodes and the screens. The influence of the gap between the screens and the edge of the focusing electrodes on the beam current is shown in Fig. 16.

On the basis of the theoretical and experimental research carried out, the aperture of the focusing electrodes was chosen equal to the aperture of the dee. Taking into consideration the need for stable and prolonged operation of the device, the gap between the screens and the electrodes was made 30 mm, and the distance from the dee to the electrodes 170 mm. In these conditions the maximum current value is reached at $U_f = -13$ kV.

In this way, as a result of the increase of the focusing forces in the central region of the accelerator, the beam current at the final radius rose from 1.1 - 1.2 to 2.1 - 2.3 $\mu$A.

In conclusion the authors wish to express their gratitude to senior technicians V.I. Ivanov and Yu V. Maximov for the construction of the 30 kV rectifier, to designer I. Kh. Nosdrin, and to K.A. Baicher, the Head of the mechanical workshop of the Laboratory for Nuclear Problems, for their great effort on the development and construction of the focusing device, and also to G.I. Selivanov, Chief engineer of the laboratory, for his great assistance in its installation.

## FIGURE CAPTIONS

Fig. 1 : Dependence of the proton beam intensity on the value of the negative voltage supplied to the dee.

Fig. 2 : Distribution of the potential in the median plane of the synchro-cyclotron at $U_f$ = 12.5 kV and $U_d$ = 1.7 kV, the value of the equi-potentials being shown in fractions of $U_f$.

Fig. 3 : Dependence of additional vertical forces on the azimuth for $U_f$ = 12.5 kV and a distance z = 0.045 m from the median plane.

Fig. 4 : Dependence of focusing forces on the radius at a distance of 4.5 cm from the median plane. 1 = magnetic forces, 2 = additional electrostatic forces at $U_f$ = - 12.5 kV.

Fig. 5 : Layout of the focusing electrodes in the acceleration chamber.

Fig. 6 : Photograph.

Fig. 7 : Dependence of the proton beam intensity on the value of the focusing voltage at various gas flow rates (for zero arc voltage).

Fig. 8 : Dependence of the proton beam intensity on the value of the focusing voltage at various gas flow rates (for several arc voltages).

Fig. 9 : Dependence of the proton beam intensity on the focusing voltage at various values of acceleration voltage.

Fig. 10 : Dependence of the proton beam current on the focusing voltage on the electrodes at various values of the negative voltage on the dee.

Fig. 11 : Dependence of proton current at a 60 cm radius on the polarity of the focusing voltage when the distance of the electrodes from the centre is 50 mm and 100 mm.

Fig. 12 : Dependence of proton-beam intensity on the focusing voltage $U_f$ when the distance between the edge of the dee and the focusing electrodes is 100, 150 and 200 mm.

Fig. 13 : Dependence of intensity on the delay in switching on acceleration voltage at various values of the voltage supplied to the focusing electrodes.

Fig. 14 : Dependence of capture time (at a level of 95% intensity) on the focusing voltage $U_f$.

Fig. 15 : Influence of the focusing voltage on the time structure of the particle beam at final radius. 1 : $U_f = 0$, 2 : $U_f = 10$ kV.

Fig. 16 : Dependence of proton beam intensity on the focusing voltage $U_f$ when distance between the electrodes and the screens is 15, 30 and 60 mm.

# REFERENCES

Литература


1. В.И. Данилов, И.Б. Енчевич, Л.Л. Новиков, Э.А. Полферов, А.Н. Сафонов, Б.В. Фектистов. Расчет начальной области устойчивых фазовых колебаний в синхроциклотроне. Препринт ОИЯИ, Р-1448, Дубна, 1963.

2. L.R.Henrich, D.C.Sewell, J.Vale. Rev. Sci. Inst., 20, 887–898 (1949).

3. R.Keller, M.Fidecaro et M.Barbier. Calcul d'orbites dans un synchro-cyclotron d'après les données techniques en considérant la charge d'espace – l'analogie avec l'oscillateur anharmonique. CERN 57-45, 1957.

4. А.Н. Сафонов, А.В. Шестов. Исследование электрического поля в центральной области синхроциклотрона ОИЯИ при помощи электролитической ванны. Б1-1543, ОИЯИ, Дубна, 1963.



Рукопись поступила в издательский отдел
21 октября 1964 г.

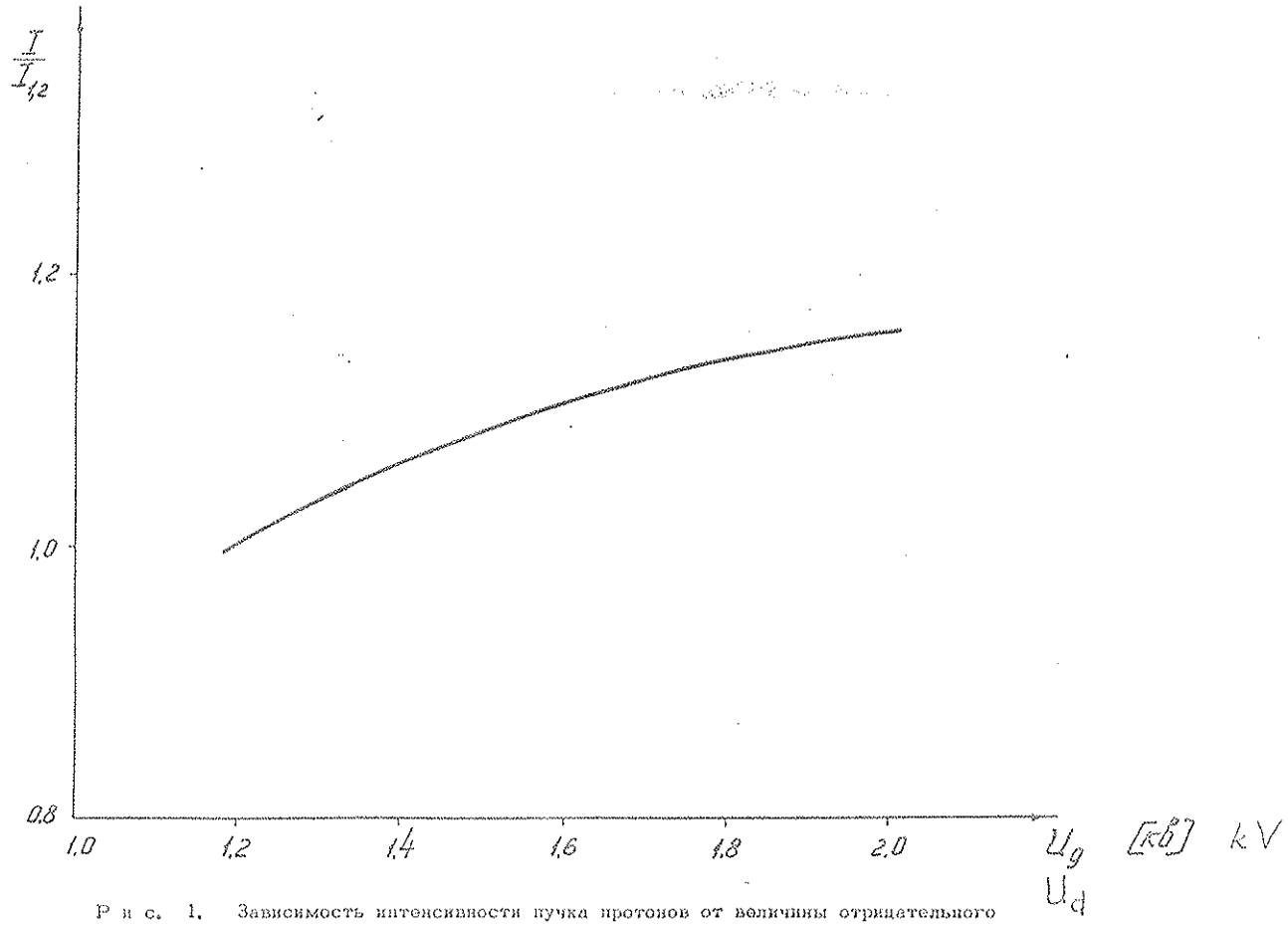


Р и с. 1. Зависимость интенсивности пучка протонов от величины отрицательного напряжения, приложенного к дуанту.



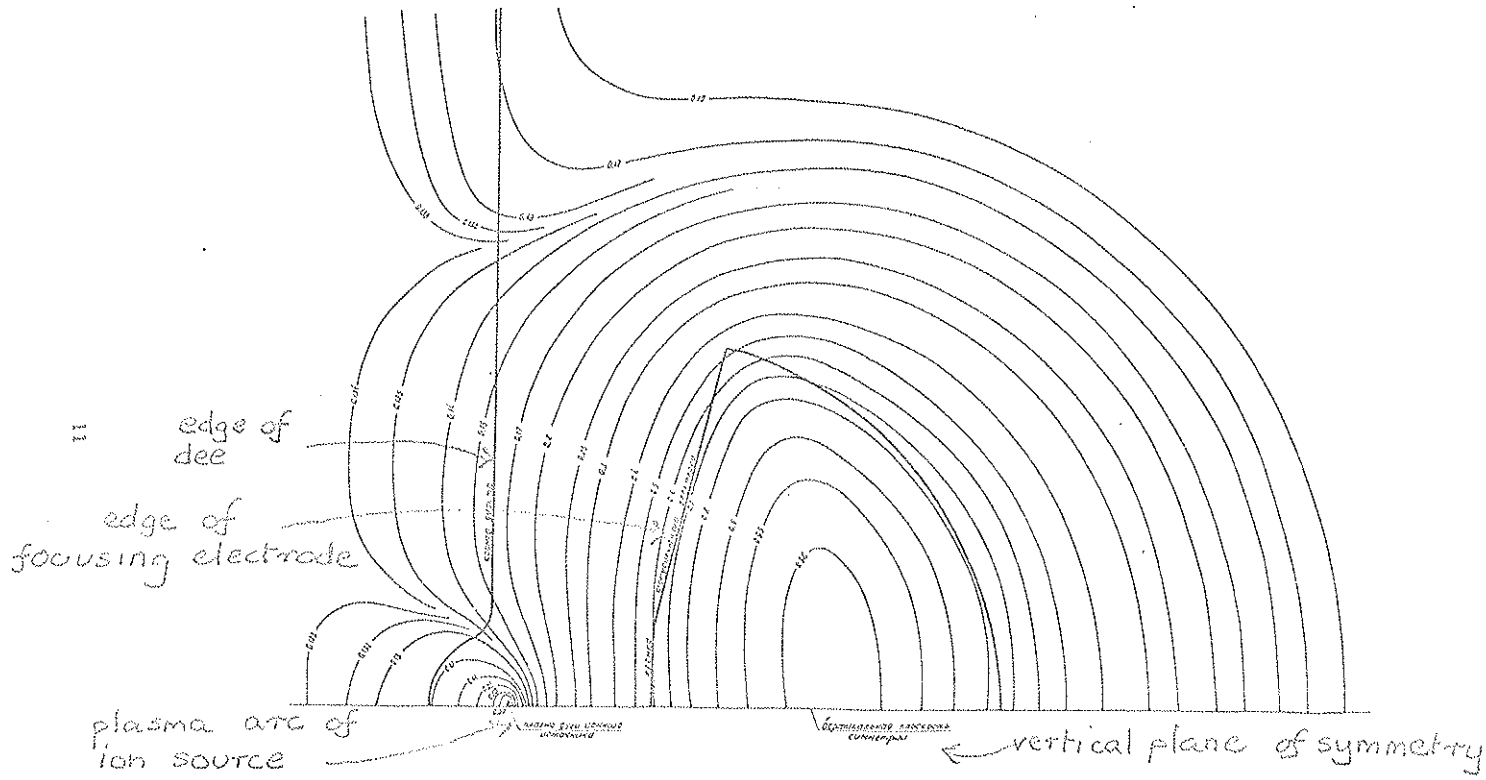


Р и с. 2. Распределение потенциала в медианной плоскости синхроциклотрона при $U_{\phi} = 12{,}5$ кв и $U_{д} = 1{,}7$ кв, значение эквипотенциалей указано в долях $U_{\phi}$.

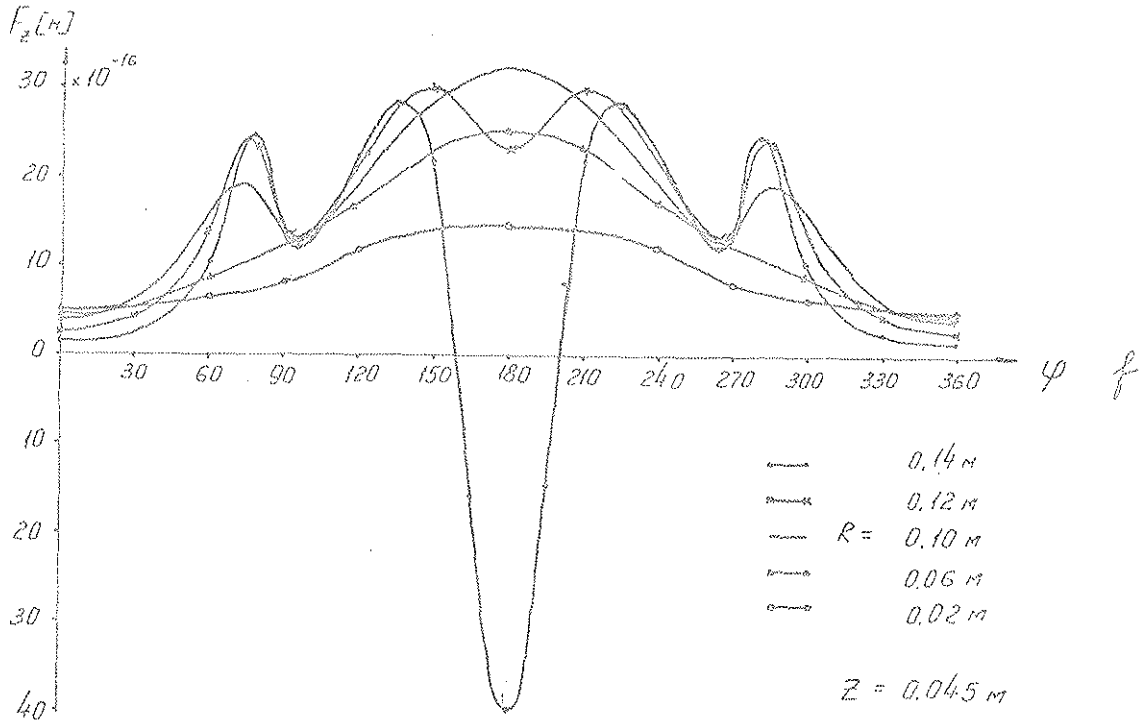


Р и с. 3. Зависимость дополнительных вертикальных сил от азимута для $U_ф$ = 12,5 кв и расстояния z = 0,045 м до медианной плоскости.

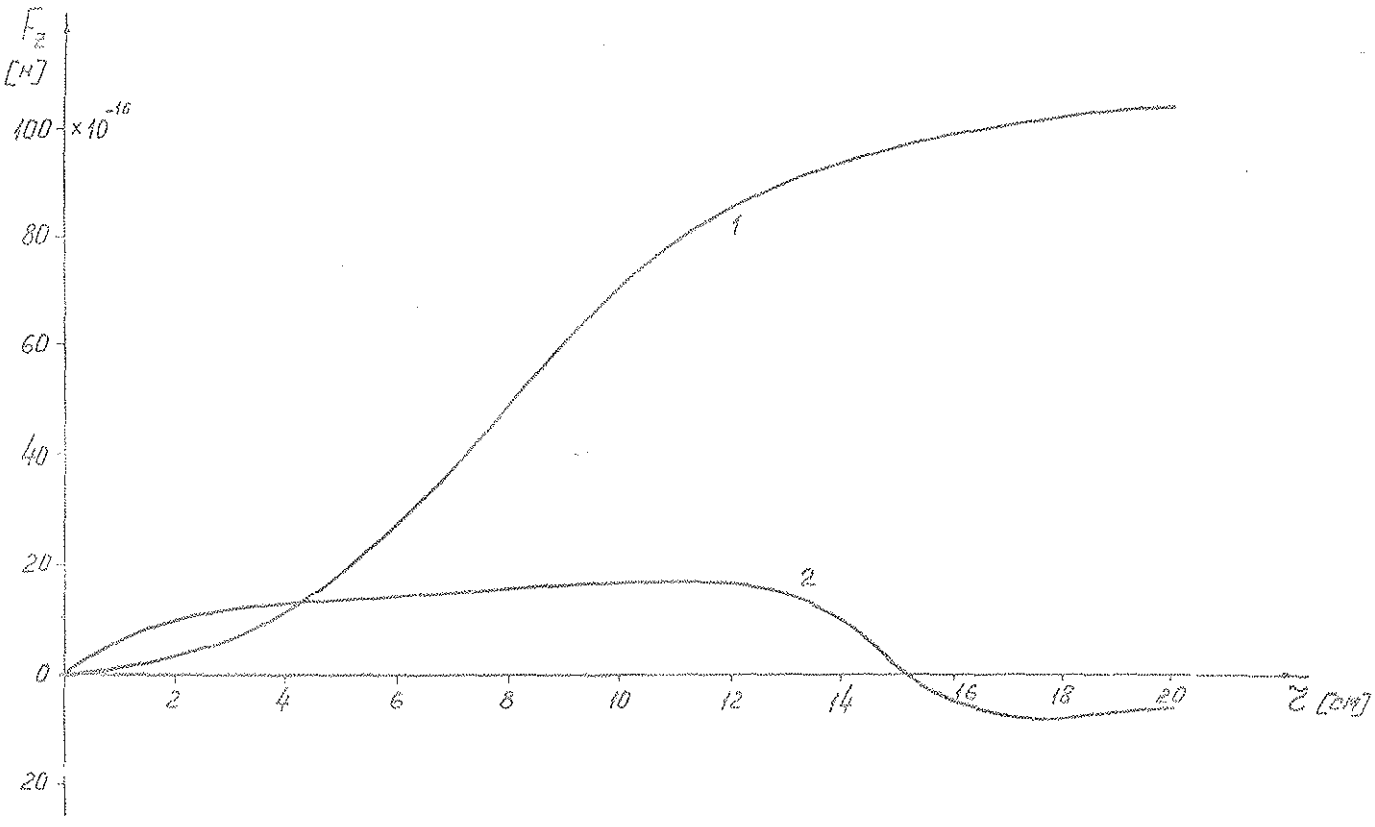


Р и с. 4. Зависимость фокусирующих сил от радиуса на расстоянии 4,5 см от медианной плоскости: 1 – магнитные силы, 2 – дополнительные электростатические силы при $U_ф$ = – 12,5 кв.

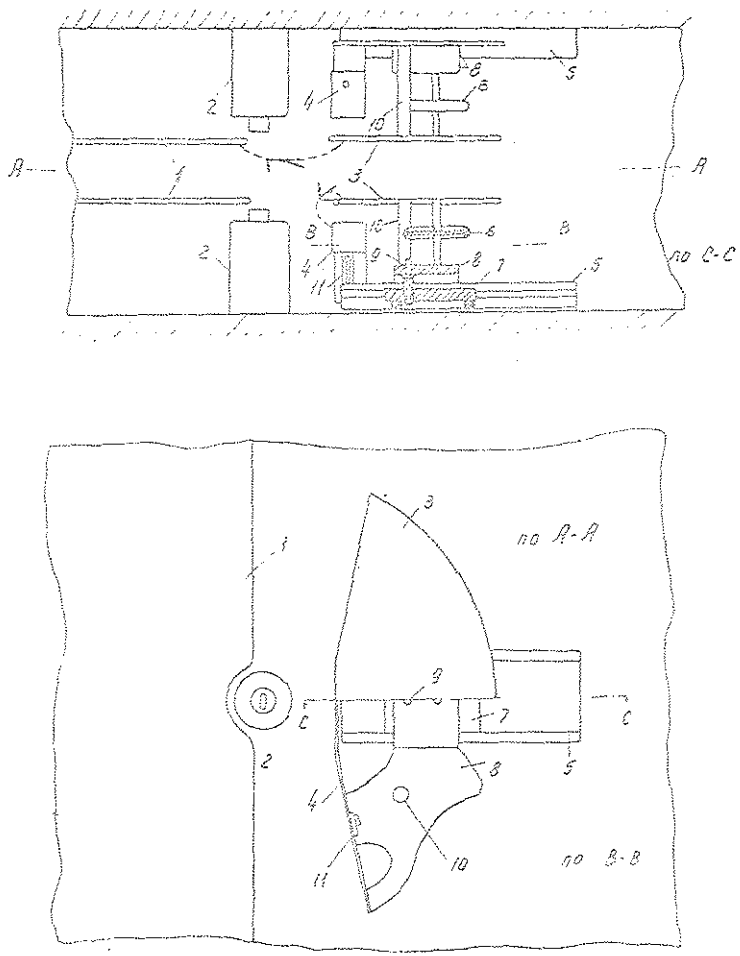


Р и с. 5. Схема расположения фокусирующих электродов в камере ускорителя.



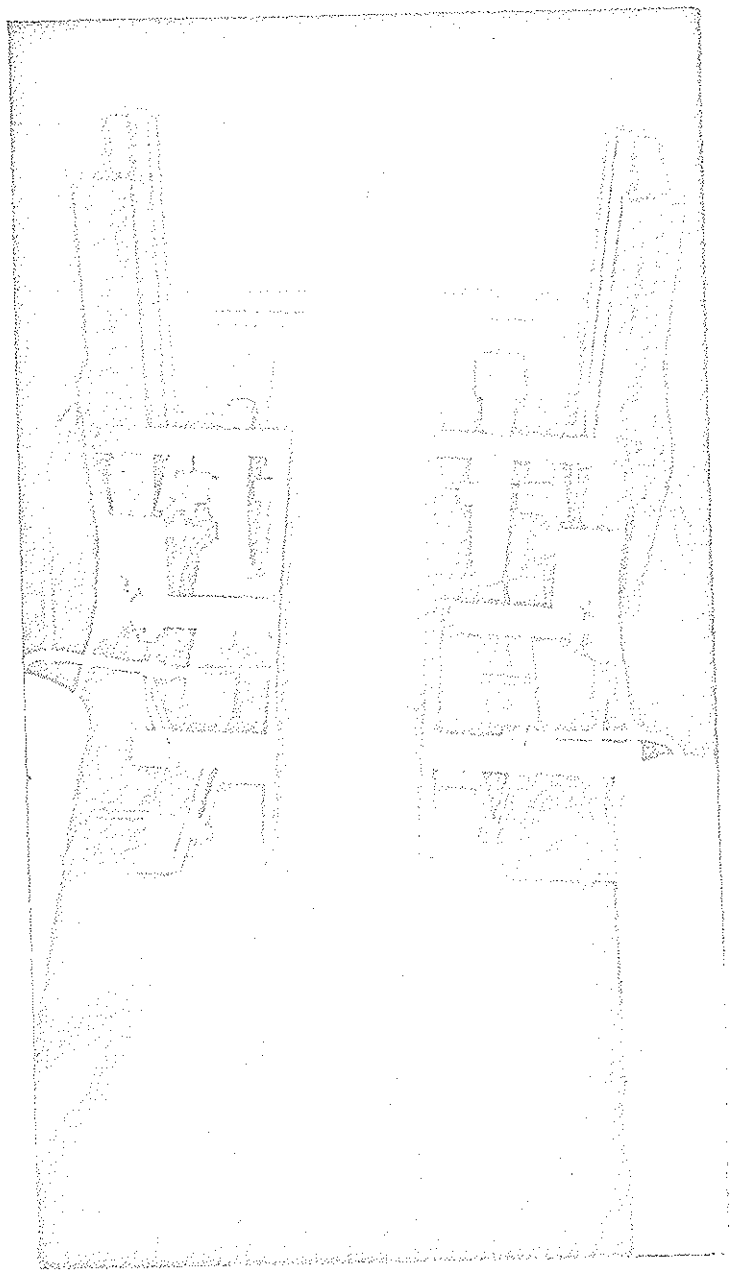

Р и с. 6.

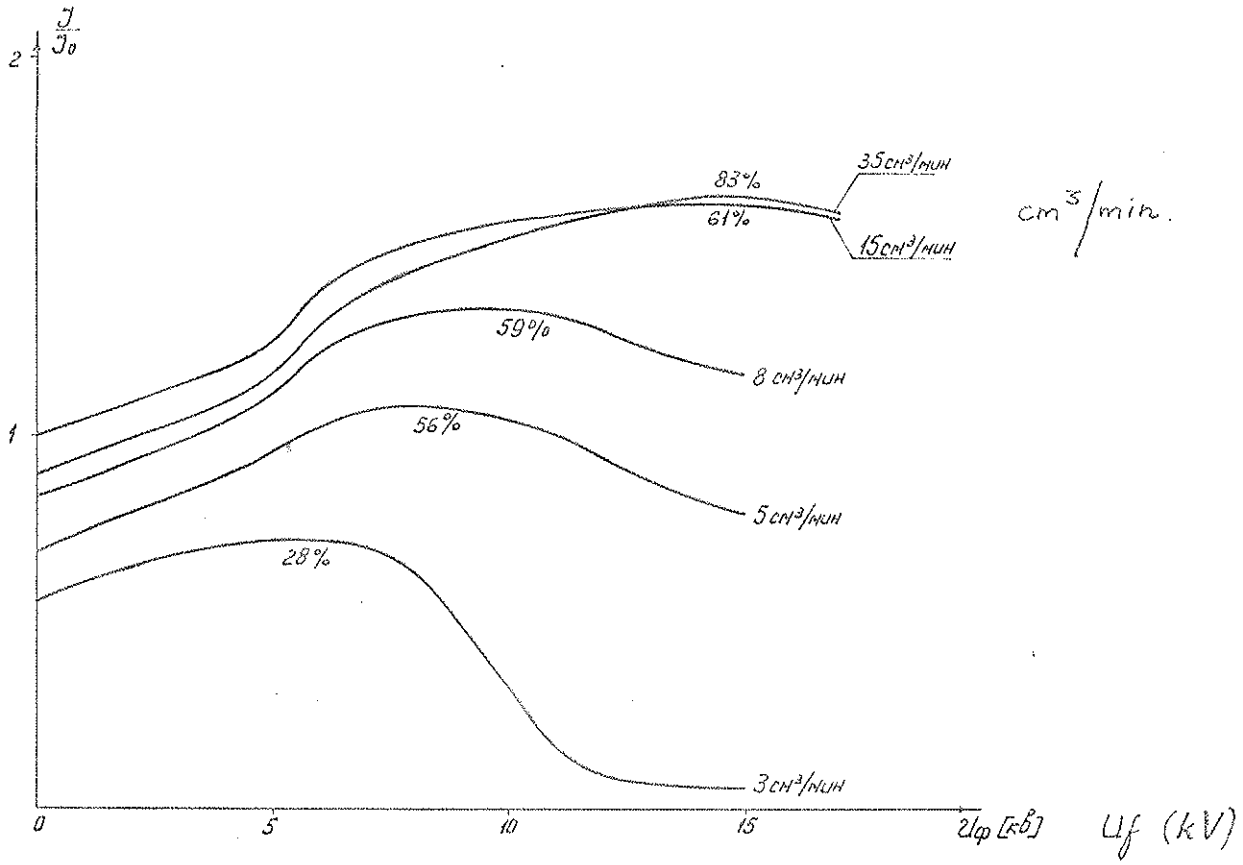


Р и с. 7. Зависимость интенсивности пучка протонов от величины фокусирующего напряжения при разном расходе газа (для нулевого напряжения дуги).



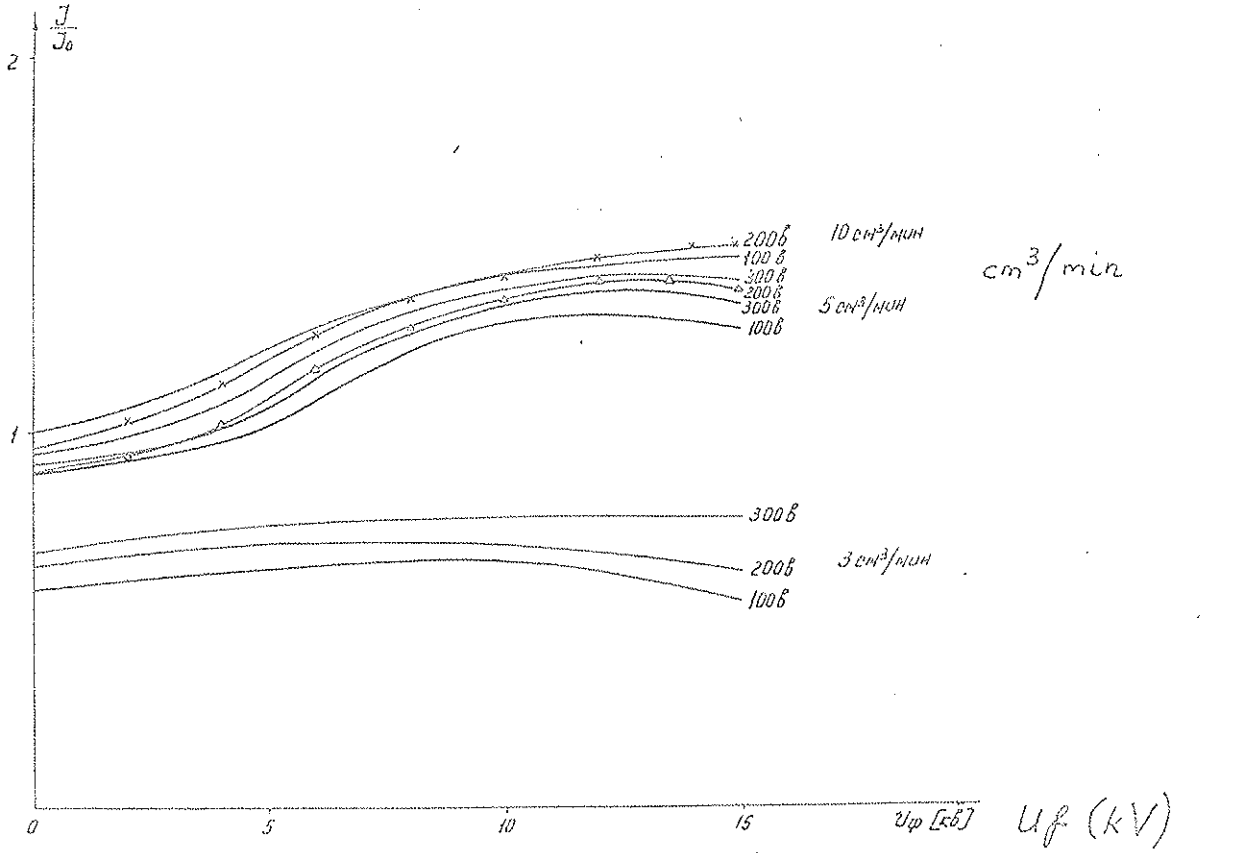


Р и с. 8. Зависимость интенсивности пучка протонов от величины фокусирующего напряжения при разном расходе газа (для нескольких напряжений дуги).

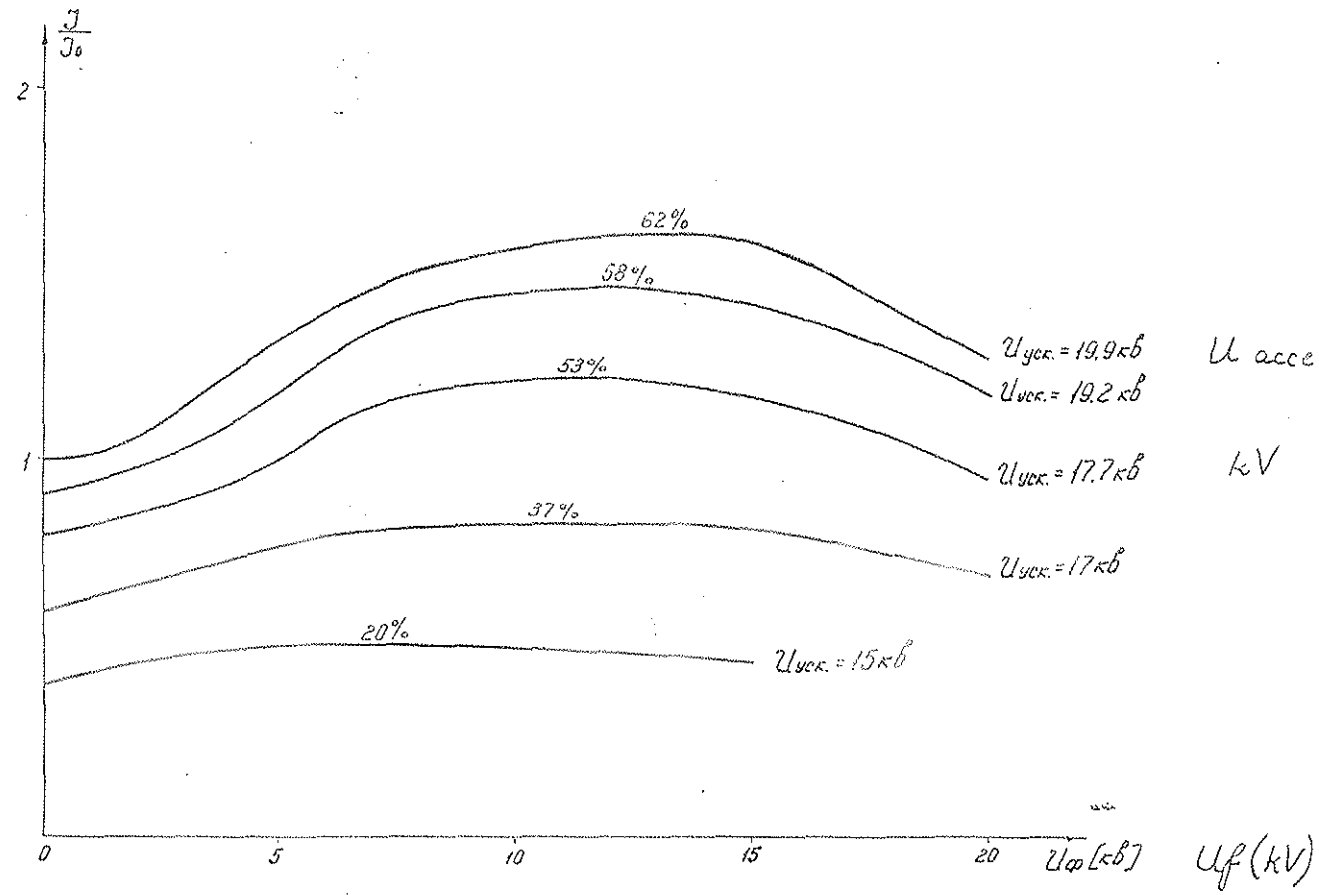


Р и с. 9. Зависимость интенсивности пучка протонов от фокусирующего напряжения для разных значений ускоряющего напряжения.

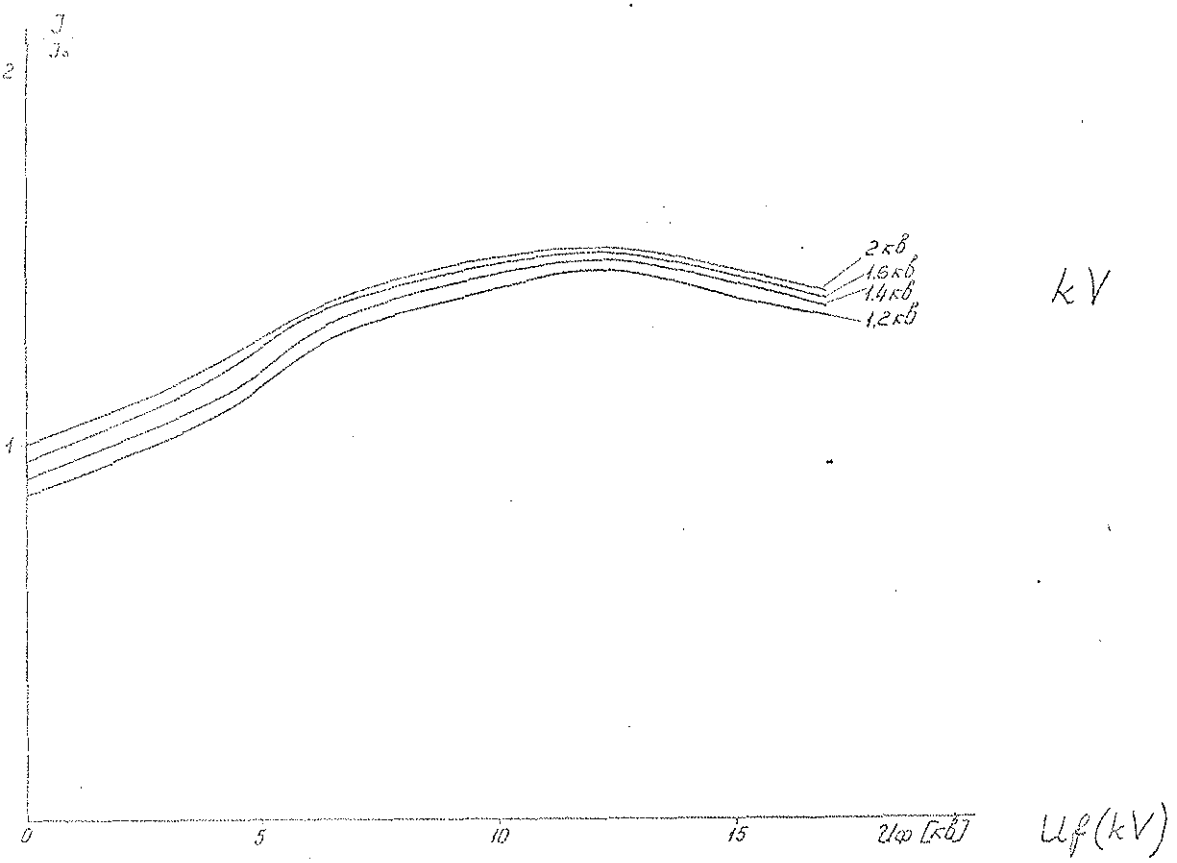


Р и с. 10. Зависимость тока пучка протонов от фокусирующего напряжения на электродах при разных значениях отрицательного напряжения на диафрагме.

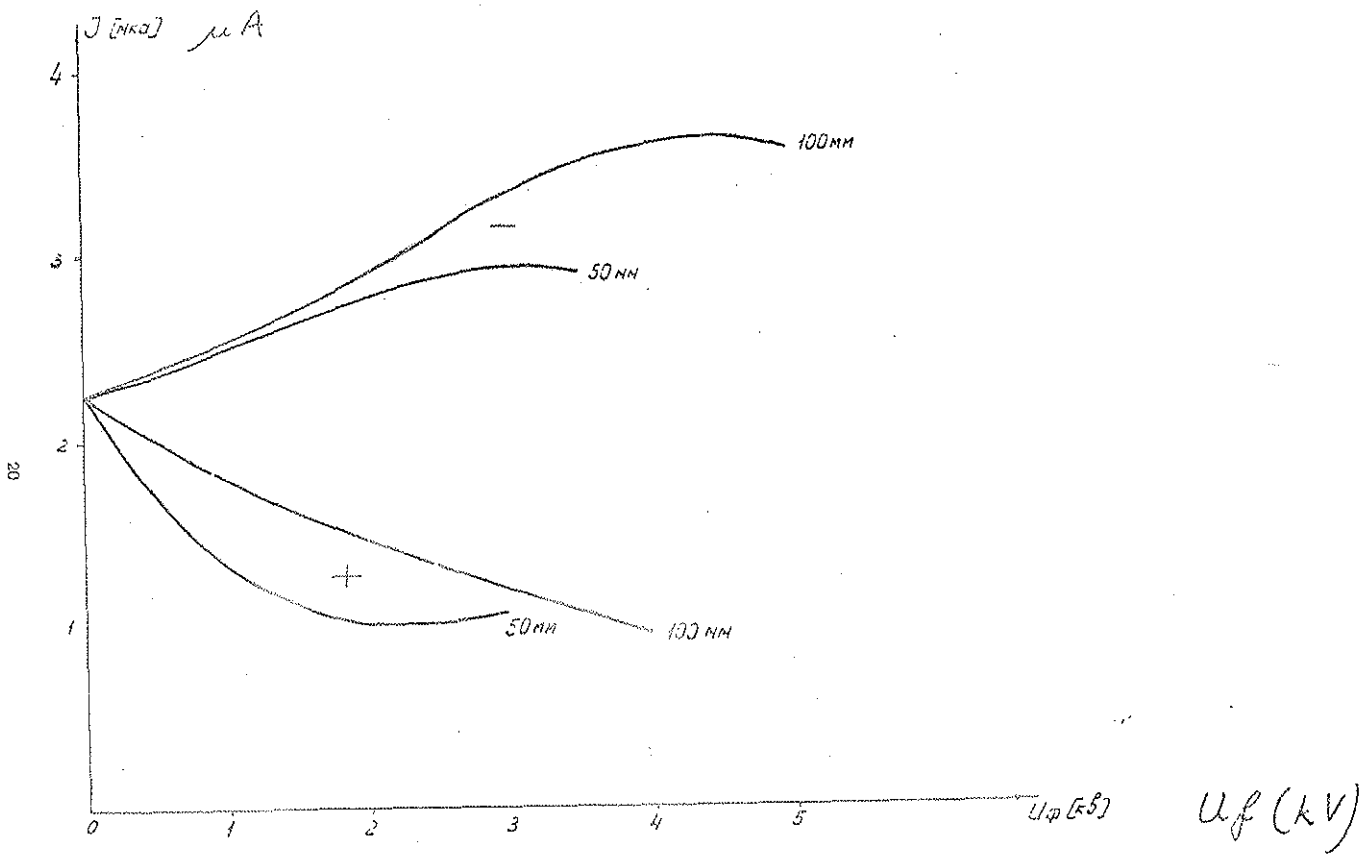


Р и с. 11. Зависимость тока протонов на радиусе 60 см от полярности фокусирующего напряжения для расстояний электродов от центра 50 мм и 100 мм.

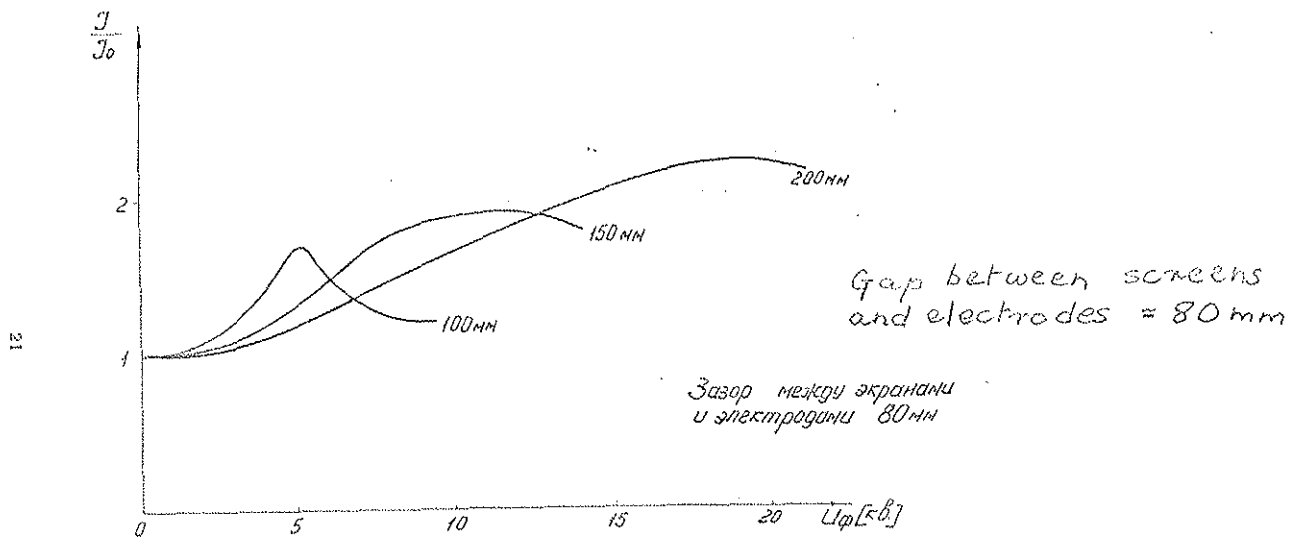


Р и с. 12. Зависимость интенсивности пучка протонов от фокусирующего напряжения $U_ф$ для расстояний между кромками дуанта и фокусирующих электродов, равных 100, 150 и 200 мм.

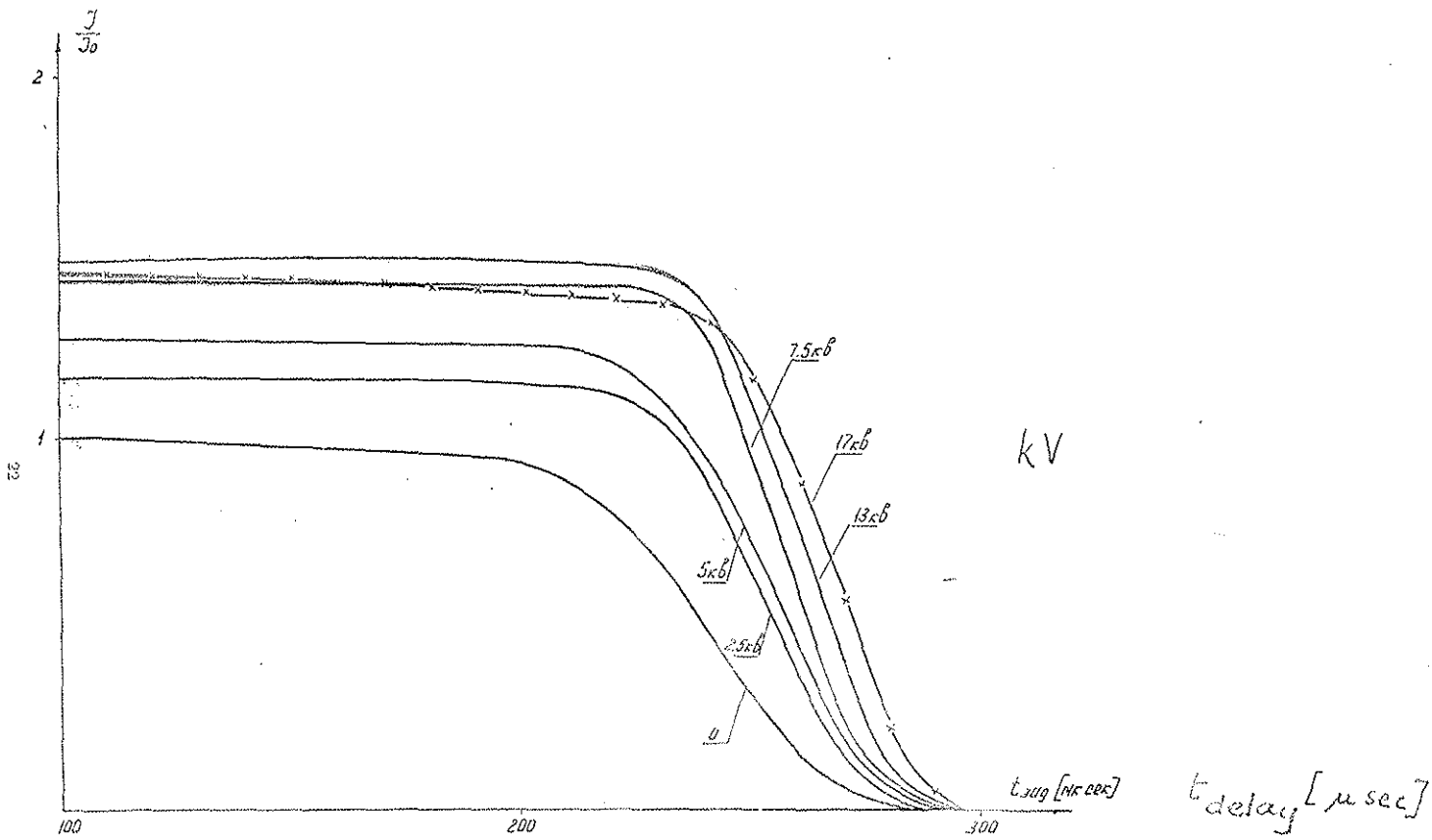


Р и с. 13. Зависимость интенсивности от величины запержки включения ускоряющего напряжения при разных значениях напряжения на фокусирующих электродах.

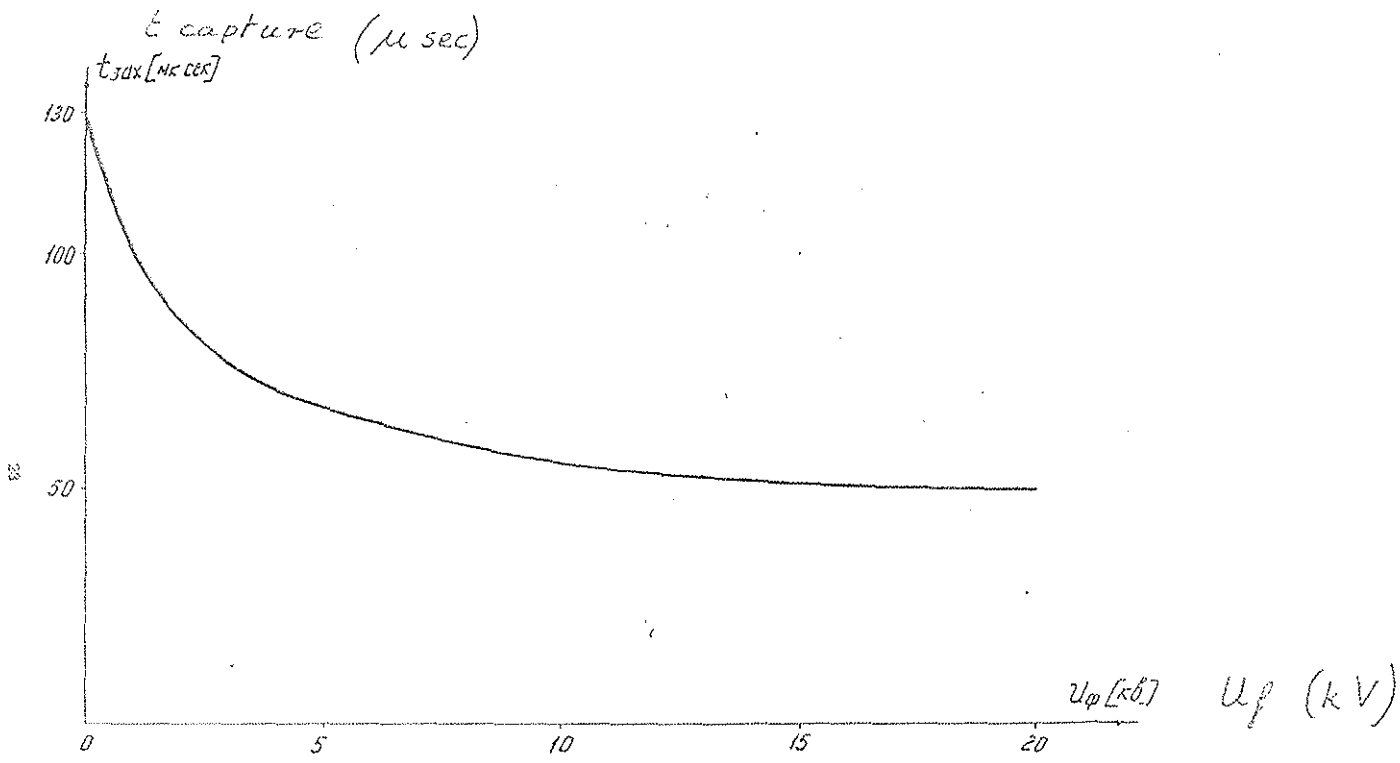


Р и с. 14. Зависимость времени захвата (по уровню 95%-ной интенсивности) от фокусирующего напряжения $U_ф$.

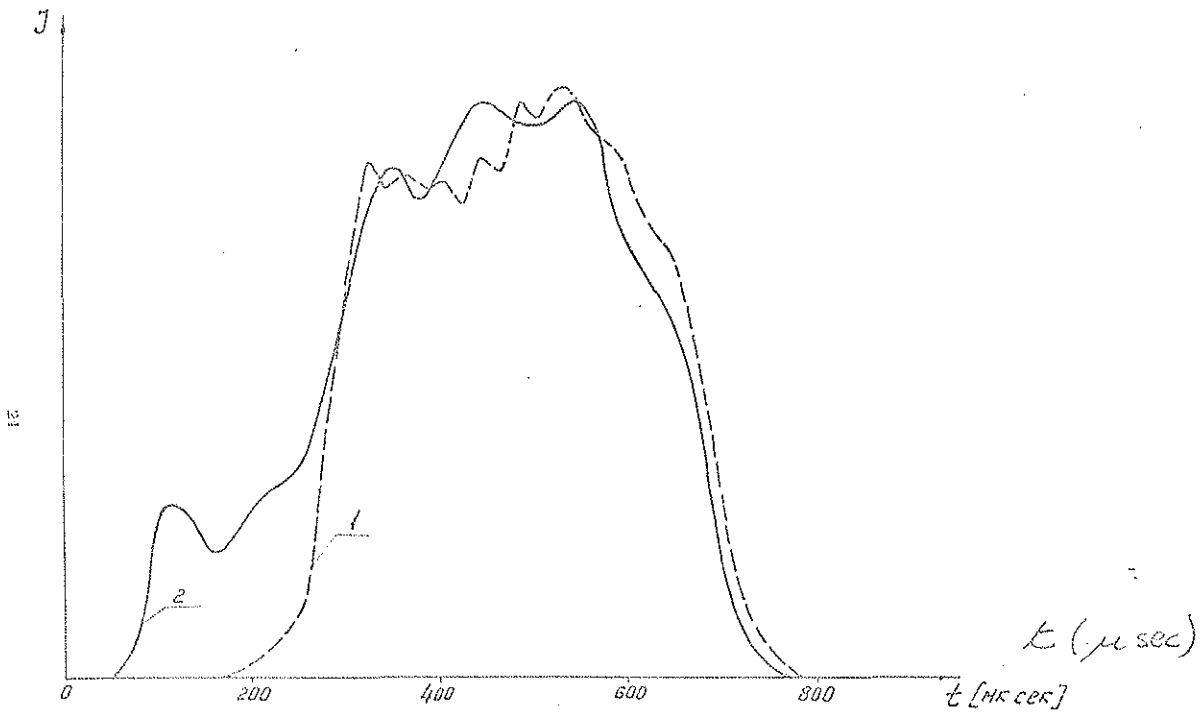


Р и с. 15. Влияние фокусирующего напряжения на временную структуру пучка частиц на конечном радиусе: 1 – $U_ф = 0$; 2 – $U_ф = 10$ кв.

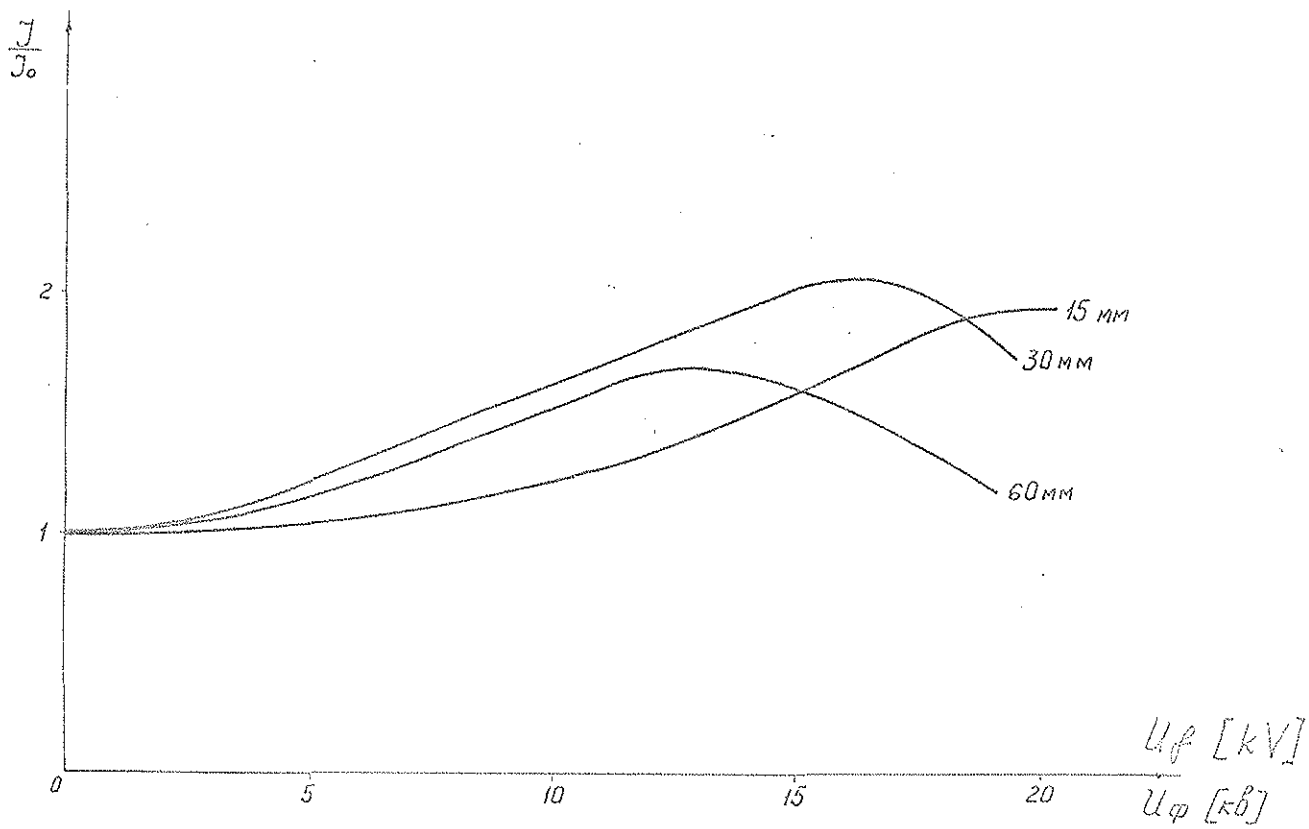


Р и с. 16. Зависимость интенсивности пучка протонов от фокусирующего напряжения $U_ф$ при зазорах между электродами и экранами, равных 15, 30 и 60 мм.